Respiratory Research

RESEARCH

Open Access

More accessible functional lung imaging: non-contrast CT-ventilation demonstrates strong association and agreement with PET-ventilation

Hilary L. Byrne[1], Nina Eikelis[2*], Jonathan Dusting[2], Andreas Fouras[2], Paul J. Keall[1] and Piraveen Pirakalathanan[2]

Abstract

Background Computed Tomography (CT) ventilation imaging (CTVI) is an emerging ventilation imaging technique. CTVI implementations have been widely validated against alternative ventilation imaging techniques but have been limited to clinical research only. The first CTVI commercial product, CT LVAS (4DMedical, Melbourne, Australia), was recently released enabling its use in clinical practice. This study quantitatively compares ventilation images from CT LVAS and previously validated research CTVI algorithms to Galligas PET ventilation.

Methods 16 patients with Galligas PET and paired inhale/exhale breath-hold CT images were taken from a publicly available dataset on The Cancer Imaging Archive. Ventilation images were produced using CT LVAS and two previously published algorithms: (1) utilising the Hounsfield Unit difference (CTVI_HU); and (2) utilising the Jacobian determinant (CTVI_Jac). CTVI images were compared to the reference standard Galligas PET using Bland-Altman analysis of lobar ventilation, voxel-wise Spearman correlation, and Dice similarity coefficient (DSC) of regions of interest representing the top 85% and 15% of ventilation function.

Results Bland-Altman analysis showed overall bias of < 0.01% for all CTVI methods (95% confidence interval: ±7.4% for CT LVAS, ± 9.1% for CTVI_HU, ± 7.9% for CTVI_Jac). The mean Spearman correlation between CTVI and Galligas PET was 0.61 ± 0.14 ($p < 0.01$) for CT LVAS, 0.68 ± 0.10 ($p < 0.01$) for CTVI_HU, and 0.57 ± 0.15 ($p < 0.01$) for CTVI_Jac. The mean DSC for the top 85% was 0.91 ± 0.03 for CT LVAS, 0.92 ± 0.02 for CTVI_HU, and 0.91 ± 0.03 for CTVI_Jac, with the DSC for CTVI_HU significantly higher than the other two CTVI methods. The DSC for the top 15% was 0.47 ± 0.17 for CT LVAS, 0.53 ± 0.16 for CTVI_HU, and 0.47 ± 0.18 for CTVI_Jac.

Conclusions In a comparison to Galligas PET ventilation imaging, CT LVAS performs similarly to previous CTVI methods. Bland-Altman analysis for quantification of lobar ventilation demonstrates negligible bias. Mean voxel-wise Spearman correlations are moderate to good. DSC of functionally thresholded lung regions are similar for all CTVI methods. These results warrant further investigation of CT LVAS as a readily available ventilation imaging tool in disease characterisation, lung health assessment, and surgical and targeted treatment planning.

*Correspondence:
Nina Eikelis
neikelis@4dmedical.com

Full list of author information is available at the end of the article

Trial registration Australian New Zealand Clinical Trials Registry (ANZCTR) registration number ACTRN12612000775819, registered on 23/07/2012.

Keywords Lung, Functional imaging, Ventilation

Background

Functional assessment in pulmonary chest imaging was developed to surpass simple structural or density-based evaluations [1]. Computational image processing methods have been developed that allow a small region of lung to be tracked across static images at known respiratory levels. X-ray velocimetry uses cross-correlation to track lung movement through a series of images taken across the breathing cycle quantifying lung expansion and has been proposed as a quantitative tool to assist or extend current lung disease diagnosis and management [2, 3]. The use of computed tomography (CT) rather than planar x-ray, allows investigation of the respiratory phase-induced change in air/tissue ratio in a small region of lung through a change in Hounsfield Unit (HU) for that region. Galbán et al. used deformably registered exhale and inhale CT images with different thresholds on each to classify lung regions affected by functional small airway disease or emphysema [4]. CT ventilation imaging (CTVI) is an emerging technology for generating 3-dimensional maps of regional lung function related to ventilation.

CTVI was first proposed as a concept by Simon [4, 5]. CT images from distinct phases of the breathing cycle, typically peak inhale and peak exhale at normal tidal volume, are deformably registered and the motion from inhale to exhale analysed to extract the local change in air volume. Development of the technique has been largely carried out with application to sparing healthy lung during radiation therapy cancer treatment where 4D CT imaging is routine standard of care [6]. However, the potential for high resolution imaging of function and the widespread availability of CT provides for the application of this technique to broader diagnostic imaging. CTVI imaging markers have been shown to be predictive of disease progression in idiopathic pulmonary fibrosis [7] and interstitial lung disease [8] and may provide an alternative to nuclear medicine techniques for imaging ventilation.

Direct methods of imaging the 3-dimensional distribution of ventilation in the lung involve imaging an inhaled gas. Single positron emission CT (SPECT) ventilation imaging is achieved through inhalation of nebulised carbon nanoparticles labelled with a gamma-ray emitter such as technetium-99 m [9, 10]. Challenges in SPECT ventilation imaging include clumping of the radiotracer, limited spatial resolution and difficulties obtaining fully quantitative imaging [11]. The inhalation of xenon gas can be used to extract a 3D image of ventilation on a dual energy CT system [12], but availability of dual energy CT systems is again limited. Positron emission tomography (PET) can also be used for ventilation imaging utilising a similar nebulised particle system radiolabelled with positron emitter gallium-68 (Galligas). PET ventilation imaging offers higher spatial resolution than SPECT and some potential improvement in clumping [13] but faces challenges of a higher capital cost and so more limited availability [14]. Magnetic resonance imaging (MRI) ventilation imaging has been demonstrated through the inhalation of a hyperpolarised gas. Despite advantages such as direct imaging of gas exchange through diffusion of the gas through the blood-gas barrier, hyperpolarised gas MRI requires specialised equipment and has extremely limited availability. The production of ventilation maps from free-breathing proton MRI [15, 16] has been investigated with promising results in several disease types, overcoming the availability and complexity challenges of hyperpolarised-gas MRI [17, 18]; however, adoption into clinical practice remains low. The logistical complexity of CT imaging without contrast is very low compared to SPECT and PET nuclear medicine scintigraphy methods and CT is more widely available than MRI, therefore CTVI holds considerable clinical value.

CTVI has been compared against these alternative methods of determining the regional distribution of ventilation. Hegi-Johnson et al. carried out a systematic review of CTVI validation against other imaging methods, concluding moderate to strong correlation at the lobar and whole-lung level [19]. An international grand challenge run through the American Association of Physicists in Medicine validated CTVI produced by entrants against three different matched imaging modalities: SPECT, Galligas PET and Xenon-CT [20]. Entries were judged using voxel-wise Spearman correlations between the CTVI and three reference standard modalities, and Dice Similarity Coefficients (DSCs) for thresholded functional segmentation of the lung. The authors concluded that further validation work and identification of a 'gold standard' imaging modality was needed, echoing the conclusions of a systematic review of functional lung imaging for radiation therapy in 2016 [21]. The development of CTVI for identifying healthy, functional lung for sparing during radiotherapy has progressed with only moderate voxel-wise correlations between modalities, but with emerging indications of utility. Application of CTVI in Phase II prospective human clinical trials of healthy lung sparing has shown positive results [22, 23], advancing the

technique toward clinical uptake in the context of radiation therapy.

Previously published CTVI techniques fall broadly into two categories, Jacobian-based methods that associate ventilation with expansion of the lung derived from a deformation vector field, and Hounsfield unit-based methods which quantify the air-tissue fraction change between deformably registered image pairs, as described in Kipritidis et al. [24]. An implementation of these two methods has been previously published in comparison to Galligas PET as a reference standard. Eslick et al. (2016) [25] compared lobar ventilation from the Hounsfield unit method only to Galligas PET and identified strong correlations in quantifying lobar function. Eslick et al. (2018) [26] used voxel-wise Spearman correlation to show that CTVI derived from breath hold CT gave better correspondence to Galligas PET ventilation than CTVI derived from 4DCT, likely due to motion artifacts affecting deformable registration accuracy.

A commercially available CT ventilation technology CT Lung Ventilation Analysis Software [CT LVAS] (4DMedical Ltd, Melbourne) has recently been released approved by the regulators in Australia and the USA, making CTVI available for clinical use. To support clinical translation of the new technology, this study assesses CT LVAS against a Galligas PET reference standard and previously validated research CTVI algorithms. For transparency and to facilitate future comparison a publicly available dataset is used. Some measures for comparing CTVI methods with Galligas PET previously published in Eslick et al. 2016 and 2018 [25, 26] have been repeated in this study to ensure results are comparable with the earlier publication as the image processing workflow differs slightly.

Methods

Ethical approval

This study utilized data from a clinical trial registered with the Australian New Zealand Clinical Trials Registry (ANZCTR) under the registration number ACTRN12612000775819, with a registration date of 23/07/2012. The clinical trial received approval from the local health district ethics committee (HREC/12/169) according to the ethical principles outlined in the Declaration of Helsinki.

Data was collected between 2013 and 2015 resulting in a publicly available dataset, 'CT-vs-PET-Ventilation-Imaging' [27] from The Cancer Imaging Archive [28]. The dataset consists of 20 matched sets of Ga-68 Galligas PET ventilation images and inhale/exhale breath-hold CT pairs obtained in the same imaging session. The ethics application status for the trial was approved, with the initial submission made on 04/07/2012 and the latest update occurring on 03/02/2022. Additionally, a data sharing statement and the trial results were provided on 03/02/2022, supporting transparency and accessibility of the trial data. The trial was prospectively registered, aligning with the standards for clinical research conduct.

Study participants

Participant characteristics and image acquisition are described in [25, 26]. In brief, lung cancer patients, 50% male, with an age range 54–73 years were imaged on a Siemens Biograph mCT.S/64 PET/CT scanner (Siemens, Knoxville USA). Galligas PET images were obtained under free-breathing conditions after inhalation of 20 MBq of 68-Ga-labelled carbon nanoparticles. Breath-hold CT (120 kV 120 mAs) were obtained with participants instructed to hold their breath at approximately 80% of maximum inhalation or exhalation. Following the results of Eslick et al. 2018 [26] showing breath hold CT gives better correlation to PET than 4DCT we have not generated CTVI from the 4DCT available in the dataset.

CT ventilation imaging and processing

CT LVAS outputs regional ventilation data derived from local measurements of lung tissue motion using three-dimensional Particle Image Velocimetry (PIV), an established image processing technique for measuring displacement vector fields with high spatial resolution (Fig. 1). As with the CTVI techniques, CT LVAS requires two thoracic CT images as inputs. These can be acquired on a standard CT instrument, without the need for contrast, and by utilizing a typical clinical paired inspiratory-expiratory CT protocol.

CTVI were also computed using two previously published algorithms: the Hounsfield Unit method (CTVI_HU) and the Jacobian method (CTVI_Jac). In both methods CT images from two breathing phases, for example inhale and exhale breath-hold CTs or two phases of a 4D-CT, are deformably registered (Fig. 1). To generate CTVI_HU, the difference in Hounsfield Unit value between each voxel of the exhale image and the deformed inhale image is calculated as described in Guerrero et al. [29] multiplied by a tissue density scaling correction accounting for the likelihood of alveolar gas exchange as described in Kipritidis et al. [30].

$$\mathrm{CTVI\_HU} = \frac{HU_{ex}(x) - HU^{*}_{in}(x+v)}{HU^{*}_{in}(x+v)+1000} \times \frac{HU\_ex(x)+1000}{1000} \quad (1)$$

Where $HU_{ex}(\boldsymbol{x})$ is the exhale CT image, $HU^{*}_{in}(\boldsymbol{x}+\boldsymbol{v})$ is the inhale CT image deformed by the vector field $\boldsymbol{v}$ and * represents a density correction applied to account for total change of mass in the lung between exhale and inhale.

To generate CTVI_Jac, following Reinhardt et al. [31] the Jacobian determinant of the deformation vector field

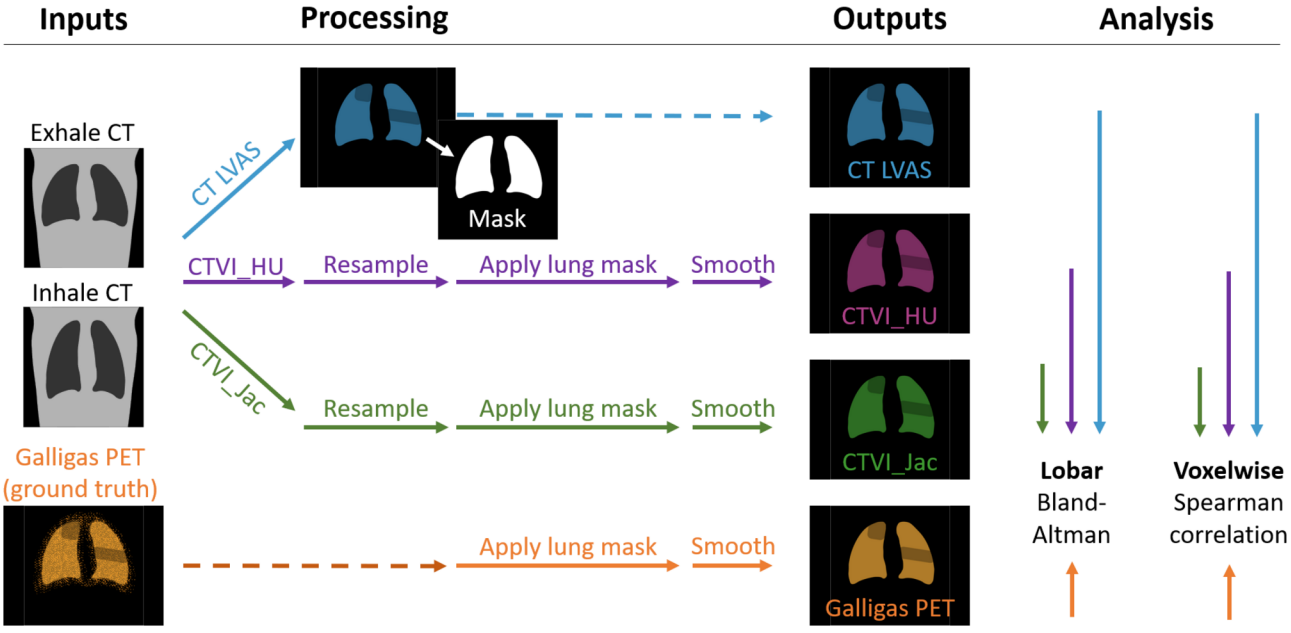

Fig. 1 Image processing steps: CT LVAS, CTVI_HU and CTVI_Jac are generated from an inhale/exhale breath-hold CT pair. CTVI_HU and CTVI_Jac are resampled to the voxel size and image dimensions of the PET image, masked to match the CT LVAS image, and a median filter of radius 3.5 voxels (7 mm) applied. The Galligas PET image is masked to match the CT LVAS image and smoothed

is computed representing the local volume expansion at each voxel. Values greater than 1 represent expansion, values from 0 to 1 represent contraction and values less than zero indicate unphysical folding. For the final ventilation metric, the Jacobian determinant is then decremented by one so that values greater than 0 represent expansion, values less than 0 represent contraction.

$$\text{CTVI\_Jac} = Jac(x, v) - 1 \tag{2}$$

Where $Jac\,(\boldsymbol{x},\ \boldsymbol{v})$ represents the Jacobian determinant of the deformation vector field $\boldsymbol{v}$ acting on the image $\boldsymbol{x}$.

Previous publications have assessed lobar ventilation correlation in this dataset [25] and the voxel-wise Spearman correlation between ventilation imaging derived from the breath-hold CT and the Galligas PET images [26]. To allow direct comparison to these earlier publications the same selection of patient data was used here– patient IDs 1 to 18, with patients 2 and 3 excluded from analysis due to a lack of motion between inhale and exhale breath-hold CTs. Patients 19 and 20 were excluded from previous analysis as their data had not been collected by the time of publication of the earlier results. Of the included patient data, three patients had undergone previous surgery, with patient ID 5 missing the right upper lobe and patients ID 10 and ID 11 missing both right middle and right lower lobes.

In this study, three CT ventilation images (CTVI) were generated for each patient from the breath-hold CT pairs using CT LVAS (4DMedical, Melbourne), the Hounsfield Unit method (CTVI_HU) and the Jacobian method (CTVI_Jac). CTVI_HU and CTVI_Jac were generated with the previously described Matlab toolkit, VESPIR [24]. All CTVI are produced in the exhale CT geometry.

CTVI_HU and CTVI_JAC were produced unmasked with voxel dimensions matching the breath-hold CT ($0.96 \times 0.96 \times 1.8$ mm^3) and were then downsampled to match the lower resolution of the PET images ($2.0 \times 2.0 \times 2.2$ mm^3) using freeware image manipulation tool Plastimatch with nearest neighbour interpolation. CT LVAS was produced for this study matching the dimensions and resolution of the PET image with lung masks applied and no further processing was carried out. The PET, CTVI_HU and CTVI_Jac were masked using the CT LVAS mask so the same voxels are identified as lung in all image modalities. Following the process in Eslick et al. [26], to reduce image noise the PET, CTVI_HU and CTVI_Jac images were smoothed using a median filter of radius 3.5 voxels, corresponding to 7 mm.

The HU method calculates a per-voxel difference in HU between the exhale and warped inhale. Taking the difference in this way can amplify CT imaging noise and smoothing is required to denoise the image. However, we note that overly smoothing the ventilation map may erode small details and potentially true ventilation signals. The 7 mm median filter was chosen to strike a balance between denoising and obscuring detail in the ventilation map. In contrast, the CTVI_Jac ventilation is drawn from the Jacobian of the deformation vector field itself which is constrained via a regularisation coefficient

to enforce smoothness of the deformations. This results in a much smoother ventilation map and further smoothing with a 7 mm median filter has a minimal effect. Similarly, the CT LVAS method is derived from an estimation of the deformation of tissue in the lung and is inherently constrained to smoothness.

Delineation of the lobes within the CT LVAS mask was carried out by experts within 4DMedical as a research service not currently available commercially. Initial lobar contours were automatically generated on the exhale breath-hold CT and then manually corrected without reference to the 4D-CT or PET images. These lobar masks were then resampled to the PET resolution for application to the final PET and CTVI images.

The lobar ventilation was calculated from the CTVI by taking the sum of the ventilation values in each voxel within the lobe divided by the sum of the ventilation values from all voxels within the lung mask, expressed as a percentage. The lobar ventilation was calculated on the PET in an analogous way by summing the activity count in each voxel within the lobe divided by the sum of the whole lung. The same lobar masks, derived from the exhale CT and resampled to the PET resolution, were used for assessment of both CTVI and PET.

The lobar ventilation for all lobes across the patient cohort was compared to Galligas PET and between the CTVI methods using a Bland-Altman analysis [32].

Correlations in the regional pattern of ventilation between CTVI and Galligas PET were assessed with methods that consider that these different modalities may measure somewhat different physiological quantities and so have a non-linear relationship. Voxel-wise Spearman correlation was used to quantify monotonicity in the ventilation information at a voxel level. Functional and high functioning lung were defined in a patient-relative fashion following the recent phase 2 clinical trial by Vinogradskiy et al. [22]. Functional lung was defined as all lung voxels excluding those voxels with a ventilation or PET activity count below the 15th percentile i.e. the top 85% of ventilation for that patient, while high functioning lung was defined as the top 15%. The Dice similarity coefficient (DSC) was used to assess overlap of the functional and high-functioning regions thus defined. Paired t-tests were used to test for significant differences in the DSC.

Results

Figure 2 shows the reference standard Galligas PET, CT LVAS, CTVI_HU and CTVI_Jac images for patient 12, selected as representative of the cohort through having a Spearman correlation to PET closest to the mean across all CTVI methods (Spearman correlation of 0.66 for CT LVAS, 0.64 for CTVI_HU, and 0.61 for CTVI_Jac). Qualitatively, a region of low function can be seen in the left lung in the Galligas PET image and all three CTVI images. Images have been normalised to the mean ventilation value or activity count within the lung mask. Normalised ventilation values greater than 3 have been assigned a value of 3, affecting less than 0.01% of voxels in CTVI_HU and CT LVAS images and no voxels in CTVI_Jac or PET images.

Visually, differences in the texture of the ventilation map can be noted between the CTVI_HU map and those based on the magnitude of tissue expansion. The HU method calculates a per-voxel difference in HU between the exhale and warped inhale, resulting in ventilation values that can differ significantly voxel to voxel. Methods based on the magnitude of expansion determined from deformation are usually regularised to enforce smoothness of the deformations. This results in a much smoother ventilation map on a spatial scale dependent on the regularisation.

Figure 3 shows the Bland-Altman plots comparing measurement of the lobar ventilation by the three CTVI methods to Galligas PET. Bland-Altman analysis showed an overall bias of $<0.01\%$ for all three methods. The 95% confidence interval was from -7.4 to 7.4% for CTVI LVAS, from -9.1 to 9.1% for CTVI_HU and from -7.9 to 7.9% for CTVI_Jac.

Figure 4 (A) shows the average ventilation across all patients in each lobe for each CTVI method. Also shown is the percentage volume occupied by each lobe. Figure 4 (B) plots the lobar ventilation from CTVI or percentage volume of each lobe for each patient against the reference standard from Galligas PET. It can be seen that for all the CTVI methods, the values lie closer to the line of equality than the lobar volume.

Figure 5 (A) shows the voxel-wise Spearman correlation comparing CT ventilation methods to the reference standard Galligas PET for each patient in the dataset. Most correlations can be defined as moderate to good (0.5–0.75) with six very good (>0.75) correlations, CTVI_Jac showing correlations between 0.25 and 0.5 for patients 16 and 17 and little relationship (Spearman correlation <0.25) between either CT LVAS or CTVI_Jac and PET for patient 13. Figure 5 (B) displays the mean voxel-wise Spearman correlations across all patients. Between CT LVAS and Galligas PET the mean Spearman correlation was found to be 0.61 ± 0.14 (range [0.17–0.80]; $p<0.01$). The Spearman correlation was 0.68 ± 0.10 (range [0.48–0.87]; $p<0.01$) between CTVI_HU and Galligas PET and 0.57 ± 0.15 (range [0.18–0.77]; $p<0.01$) between CTVI_Jac and Galligas PET.

The correlation between the CT ventilation methods was 0.65 ± 0.12 (range [0.31–0.81]; $p<0.01$) between CT LVAS and CTVI_HU, 0.73 ± 0.07 (range [0.60–0.83]; $p<0.01$) between CT LVAS and CTVI_Jac, and 0.68 ± 0.12 (range [0.35–0.82]; $p<0.01$) between CTVI_HU and CTVI_Jac.

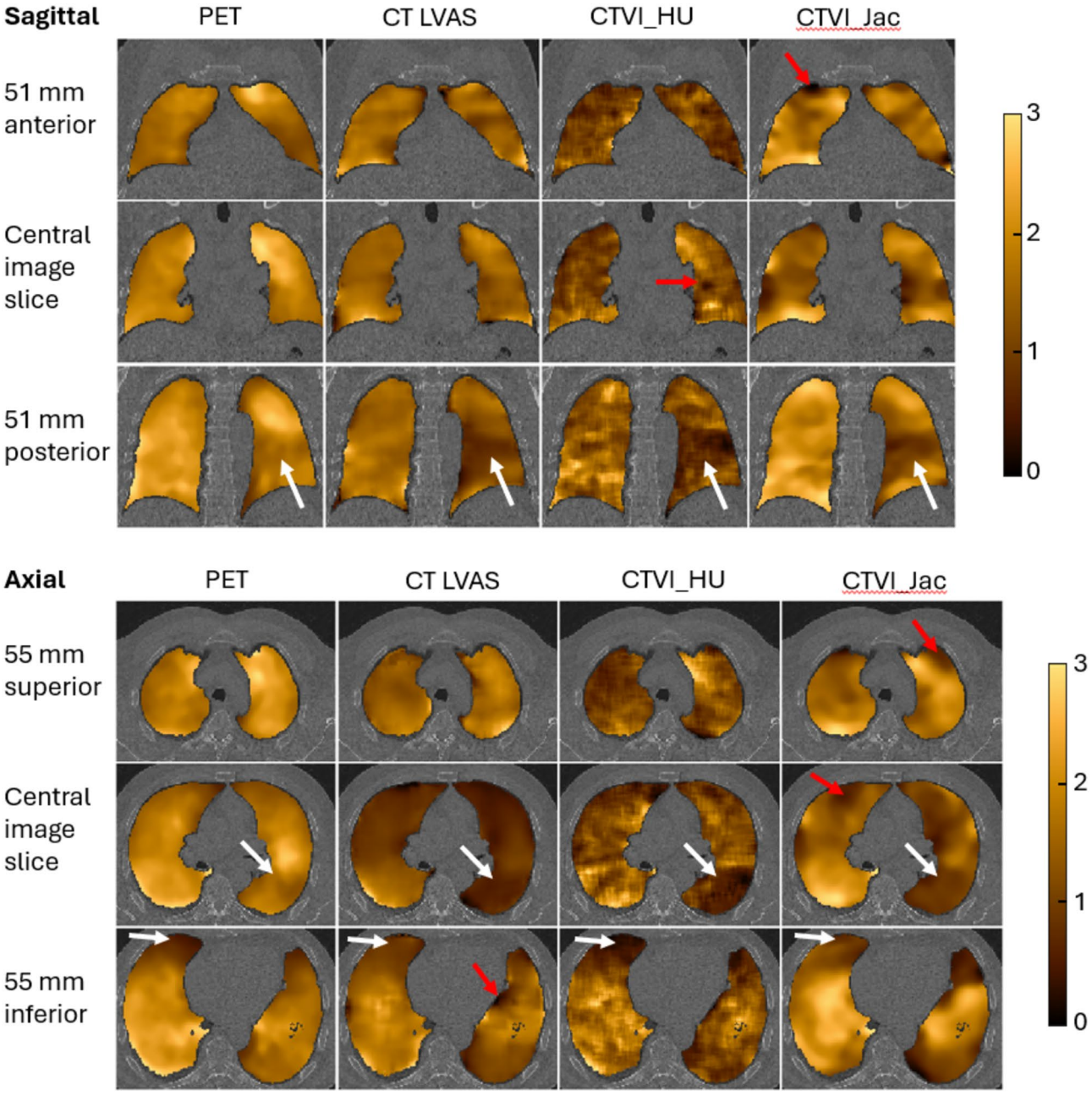

Fig. 2 Ventilation images for patient 12, chosen as representative of the mean Spearman correlation between the CTVI modalities and Galligas PET. Images are normalised to the median ventilation value within the lung mask. Regions of visibly lower activity on the PET image with corresponding low functioning regions on the CTVI are marked with white arrows. Some areas visibly appear to be mismatched - indicative areas of low ventilation on CTVI that do not appear on other modalities have been indicated with red arrows

Functional lung regions were segmented by threshold to represent functional lung (the top 85%of lung function) and high functioning lung (the top 15% of lung function). The mean DSCs for functional and high functioning lung between the CTVI and Galligas PET, and between different CTVI modalities, are shown in Table 1.

A repeated measures ANOVA with Tukey's multiple comparisons test (GraphPad Prism v10.2.1) was used to test for significant differences in the DSCs in Table 1. It is of interest to ask if one of the three CTVI methods shows a higher Dice score to PET than the other CTVI methods. The CTVI_HU to PET DSC is significantly higher than CT LVAS to PET ($p<0.05$) and CTVI_Jac to PET ($p<0.005$) for high functioning lung but there are no significant differences for low functioning lung indicating similar performance relative to the reference standard for all three methods in identifying ventilation defects in this small cohort of lung cancer patients. Statistical

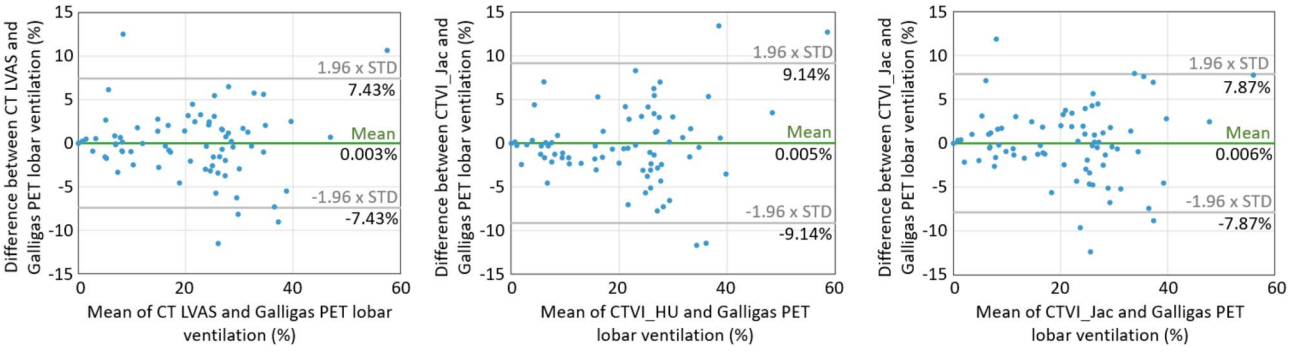

Fig. 3 Bland-Altman plots of CT LVAS, CTVI_HU and CTVI_Jac vs. PET lobar ventilation, plotting the average of the CTVI method and PET (x-axis) against the difference (y-axis)

significance for the functional lung region has not been assessed as the magnitude of difference between the mean DSCs is very small.

Discussion

This study compared the lobar and 3-dimensional distribution of ventilation produced by CT LVAS to a PET Galligas ventilation reference standard and previously published CTVI algorithms. The results of the current study indicate the CT LVAS performs comparably to previously published CT ventilation algorithms, with moderate to good correlation between the CTVI and Galligas PET lung ventilation imaging at a lobar level and moderate correlation in a voxel-wise comparison. The Bland-Altman analysis indicates agreement in predicting lobar percentage ventilation between CT LVAS and Galligas PET within around 5% ventilation. Agreement between the ventilation methods is better than the agreement between lobar percentage volume and Galligas PET indicating that lung function is not evenly distributed across the lung parenchyma.

Figure 2 indicates that broad patterns of ventilation defect may be visible in all the ventilation methods explored here while also highlighting there can still be discrepancies between methods. We note that in methods using deformable image registration the accuracy of the ventilation measure will be directly related to the quality of the registration. The supplementary information gives more examples of ventilation imaging from all modalities for both high and low Spearman correlations including cases 13 and 16 where there is discrepancy between the CTVI methods. Without clinical information provided with the dataset no conclusions can be drawn as to which method is in fact more accurate. The clinical utility of spatial ventilation mapping and the significance of these differences between methods will likely need to be determined on a disease-specific or clinical application basis.

The analysis here differs from that in Eslick et al. (2018) [26] in adding CTVI_Jac to the lobar analysis and in the use of the CT LVAS lung mask rather than one generated by the VESPIR Matlab toolkit used in that publication. Therefore, Spearman correlations were recalculated to allow comparison between the CTVI methods. The voxel-wise Spearman correlation found here for CTVI_HU (0.68 range [0.48–0.87]) and CTVI_Jac (0.57 range [0.18–0.77]) are similar to those found by Eslick et al.: 0.67 (range: 0.52–0.87) and 0.57 (range: 0.18–0.77) respectively indicating the change in analysis has only a small impact.

Perfect correlations between CTVI and Galligas PET should not be expected as there are several sources of potential discrepancy. The two methods use different surrogate physical processes to estimate ventilation. Galligas PET uses the inhalation of particles which adhere to airway surfaces and can be affected by turbulent or disrupted airflows, airway surface characteristics and clumping behaviour. CTVI on the other hand measures tissue expansion or air/tissue ratio change as surrogates of ventilation. In addition, the Galligas PET is a time-average of ventilation with the patient breathing freely to tidal volume while the CT images, although captured at the same imaging session, are from separate breath hold manoeuvres without spirometric confirmation of lung expansion state.

It is known that differences in patient inhalation depth lead to differences in patterns of ventilation and reduced ventilation heterogeneity [33–37] as do differences in patient setup between prone and supine positioning [38]. The inhalation instruction given to patients for this dataset (80% of maximum inhale) as detailed in Eslick et al. 2018 [26] is non-standard. However it is not clear what the optimal inspiratory volume would be for CTVI. Larger volumes may give less noise in a surrogate ventilation signal dependent on expansion or air-tissue ratio change, but may not be representative of the clinically important ventilation. CTVI may also vary with chosen scan parameters. No study has yet systematically investigated the effect of different CT scan parameters on the ventilation map produced.

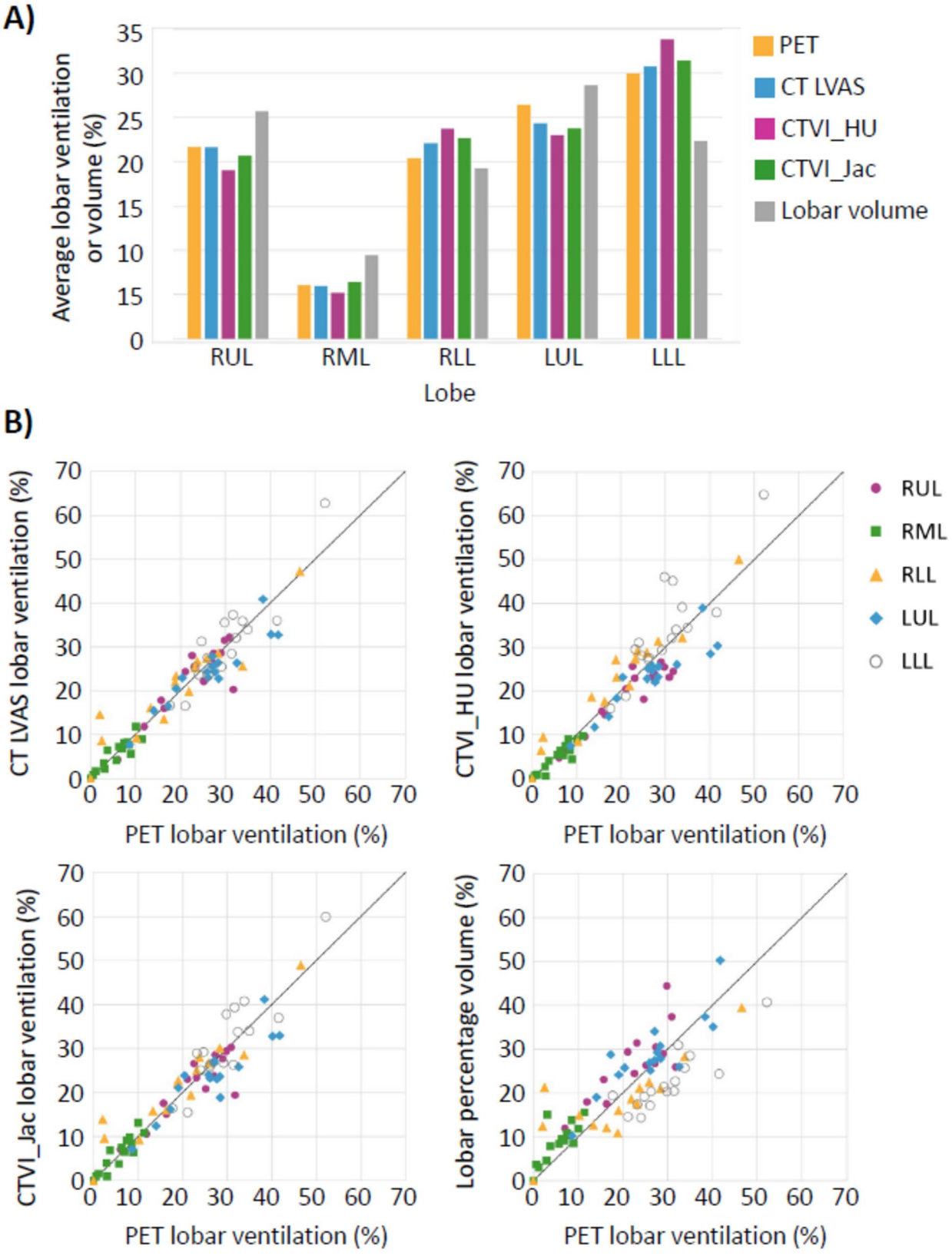

Fig. 4 **A**) Histogram showing the lobar ventilation from each CTVI method and the percentage volume in each lobe. **B**) Plots of the lobar ventilation from the reference standard Galligas PET against each CTVI method and the lobar percentage volume. RUL: right upper lobe; RML: right middle lobe; RLL: right lower lobe; LUL: left upper lobe; LLL: left lower lobe

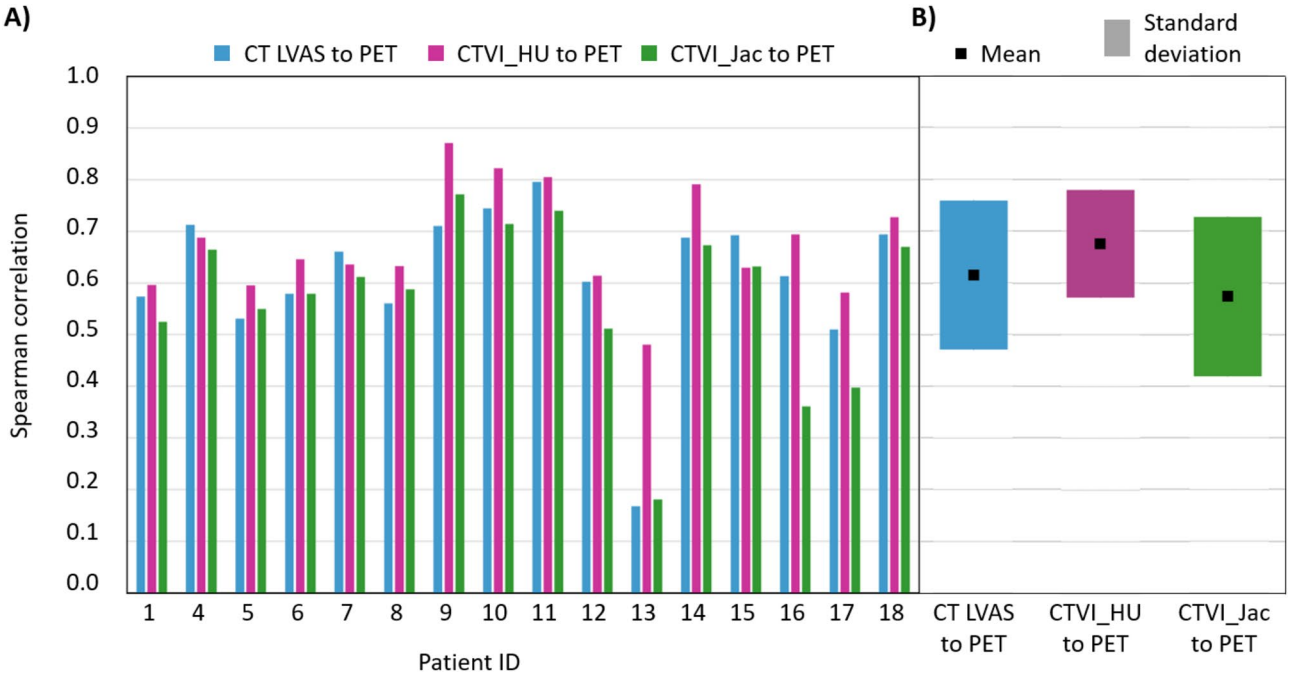

Fig. 5 Voxel-wise Spearman correlations between CTVI methods and Galligas PET, **A**) for each patient and **B**) mean and standard deviation for each method

Table 1 Mean dice similarity coefficients across all patients for functional lung (representing the top 85% of lung function), high functioning lung (representing the top 15% of function) and low functioning lung (representing the bottom 15% of function) between CTVI and the reference standard Galligas PET, and between different CTVI methods

	CT LVAS to Galligas PET	CTVI_HU to Galligas PET	CTVI_Jac to Galligas PET	CT LVAS to CTVI_HU	CT LVAS to CTVI_Jac	CTVI_HU to CTVI_Jac
Functional Lung (top 85%)	0.91 ± 0.03	0.92 ± 0.02	0.91 ± 0.03	0.91 ± 0.02	0.92 ± 0.02	0.91 ± 0.02
High functioning lung (top 15%)	0.47 ± 0.17	0.53 ± 0.16	0.47 ± 0.18	0.57 ± 0.15	0.66 ± 0.10	0.61 ± 0.15
Low functioning lung (bottom 15%)	0.52 ± 0.15	0.57 ± 0.14	0.48 ± 0.17	0.50 ± 0.13	0.49 ± 0.12	0.57 ± 0.11

Figure 4 suggests that CTVI ventilation approximates the PET ventilation closer than the simple lobar volume. However, it appears to show a systematic under-ventilation of the upper lobes and over-ventilation of the lower lobes compared to the lobar volume. This could be a sign of systematic differences introduced by differences in lung inflation state. The lobar volumes are defined on the exhale CT, and while the CTVI are produced in the exhale geometry they use motion/change between the exhale and inhale. The PET is again different as an average over the breathing cycle. If lobar volume change is not linear with lung inflation state a systematic bias could be introduced comparing ventilation to volume at different inflation states. However, in addition, patients in the dataset have very heterogenous lung function with signs of emphysema, late stage lung cancer physically blocking ventilation to entire lobes and previous surgeries. It is also possible that the systematic differences seen here would not be borne out in a larger cohort of patients. Further investigation is needed and would be ideally carried out in healthy patients to test for systematic bias in the absence of large ventilation heterogeneities.

As seen in Fig. 2, discrepancies are visible between all the ventilation methods explored here. Previous studies have related CTVI of defects to pathological results of the physical lung condition in small animals, but this is generally hard to achieve in human clinical trial. The clinical utility of spatial ventilation mapping and the significance of these differences between methods will likely need to be determined on a disease-specific or clinical application basis.

No diagnostic information was available for the patient cohort studied here so this study is limited to demonstrating the technical equivalence of CT LVAS with other ventilation measures. Where disagreement occurs between the methods this study is unable to relate one method to better determination of clinical outcomes. Future work must determine the suitability of CTVI for clinical application, including consideration of how sensitive it is to the known dependency of patterns of ventilation on the

inspiration volume [36, 39] and potential impact of varying scan parameters and imaging dose on the quality and accuracy of produced ventilation images.

CT imaging without contrast is affordable and readily available in most centres, offering an alternative where nuclear imaging is unavailable, cost prohibitive, or there are contraindications to its use. Giving a regional measure of ventilation, CT LVAS has potential application to general lung health assessment, disease diagnosis, monitoring progression and treatment response, and surgical or targeted treatment planning.

Conclusions

In a comparison to Galligas PET ventilation imaging, CT LVAS performs similarly to previous CTVI methods. Bland-Altman analysis for quantification of lobar ventilation demonstrates negligible bias and confidence intervals of less than ±10%. Mean voxel-wise Spearman correlations are moderate to good. Dice similarity coefficients of functionally thresholded lung regions are similar for all CTVI methods. These results warrant further investigation of CT LVAS as a readily available ventilation imaging tool in disease characterisation, lung health assessment, and surgical and targeted treatment planning.

Abbreviations

CT	Computed tomography
CTVI	Computed tomography ventilation imaging
CT LVAS	Computed tomography lung ventilation analysis software
DSC	Dice similarity coefficient
HU	Hounsfield unit
Jac	Jacobian determinant
PET	Positron emission tomography
SPECT	Single photon emission computed tomography

Supplementary Information

The online version contains supplementary material available at https://doi.org/10.1186/s12931-025-03245-2.

Supplementary Material 1

Acknowledgements

The authors would like to acknowledge assistance from Punit Shah in providing CT LVAS ventilation images.

Author contributions

HB, NE and PP conceived and designed the idea and analysis for the manuscript. HB performed the image processing, gathered and analysed data and took the lead in drafting the manuscript. HB, NE, JD, AF, PK and PP discussed the study design, commented on the analysis method, and read, edited and approved the final manuscript.

Funding

This research has been supported by a Cancer Institute NSW Translational Program Grant 2019/TPG2165.

Data availability

No datasets were generated or analysed during the current study.

Declarations

Ethics approval and consent to participate

This study uses data from a prospective single institution clinical trial approved by the health district ethics committee (HREC/12/169) and registered with the Australian New Zealand Clinical Trials Registry (ACTRN12612000775819, registration date 23/07/2012). The study was approved by the Northern Health Human Research Ethics Committee on 21/03/2013 (Ethics approval number 1206-175 M).

Consent to participate and Consent

To Publish is not applicable for this retrospective study.

Competing interests

NE, JD, AF, PP are employees of 4DMedical Ltd which produces the CT LVAS product.PK is an inventor on a licenced patent on CT ventilation imaging. HB received an Australian Government fellowship (REDIF147) to carry out work presented in this manuscript.

Author details

[1]Image X Institute, Sydney School of Health Sciences, Faculty of Medicine and Health, The University of Sydney, Sydney, Australia
[2]4DMedical Ltd, Melbourne, Australia

Received: 21 October 2024 / Accepted: 18 April 2025
Published online: 26 April 2025

References

1. Maki DD, Gefter WB, Alavi A. Recent advances in pulmonary imaging. Chest. 1999;116(5):1388–402.
2. Siddharthan T, Grealis K, Kirkness JP, Ötvös T, Stefanovski D, Tombleson A, et al. Quantifying ventilation by X-ray velocimetry in healthy adults. Respir Res. 2023;24(1):215.
3. Karmali D, Sowho M, Bose S, Pearce J, Tejwani V, Diamant Z et al. Functional imaging for assessing regional lung ventilation in preclinical and clinical research. Front Med [Internet]. 2023 May 16 [cited 2024 Jul 11];10. Available from: https://www.frontiersin.org/journals/medicine/articles/https://doi.org/10.3389/fmed.2023.1160292/full
4. Simon BA. Regional ventilation and lung mechanics using X-Ray CT. Acad Radiol. 2005;12(11):1414–22.
5. Simon BA. Non-Invasive imaging of regional lung function using X-Ray computed tomography. J Clin Monit Comput. 2000;16(5):433–42.
6. Vinogradskiy Y. CT-based ventilation imaging in radiation oncology. BJR|Open. 2019;1(1):20180035.
7. Scharm SC, Vogel-Claussen J, Schaefer-Prokop C, Dettmer S, Knudsen L, Jonigk D, et al. Quantification of dual-energy CT-derived functional parameters as potential imaging markers for progression of idiopathic pulmonary fibrosis. Eur Radiol. 2021;31(9):6640–51.
8. Scharm SC, Schaefer-Prokop C, Willmann M, Vogel-Claussen J, Knudsen L, Jonigk D, et al. Increased regional ventilation as early imaging marker for future disease progression of interstitial lung disease: a feasibility study. Eur Radiol. 2022;32(9):6046–57.
9. Bajc M, Neilly B, Miniati M, Mortensen J, Jonson B. Methodology for ventilation/perfusion SPECT. Semin Nucl Med. 2010;40(6):415–25.
10. Roach PJ, Schembri GP, Bailey DL. V/Q scanning using SPECT and SPECT/CT. J Nucl Med. 2013;54(9):1588–96.
11. Petersson J, Sánchez-Crespo A, Larsson SA, Mure M. Physiological imaging of the lung: single-photon-emission computed tomography (SPECT). J Appl Physiol. 2007;102(1):468–76.
12. Kong X, Sheng HX, Lu GM, Meinel FG, Dyer KT, Schoepf UJ, et al. Xenon-Enhanced Dual-Energy CT lung ventilation imaging: techniques and clinical applications. Am J Roentgenol. 2014;202(2):309–17.
13. Le Roux PY, Hicks RJ, Siva S, Hofman MS. PET/CT lung ventilation and perfusion scanning using Galligas and Gallium-68-MAA. Semin Nucl Med. 2019;49(1):71–81.
14. Bailey DL, Eslick EM, Schembri GP, Roach PJ. 68Ga PET ventilation and perfusion lung Imaging—Current status and future challenges. Semin Nucl Med. 2016;46(5):428–35.
15. Bauman G, Puderbach M, Deimling M, Jellus V, Chefd'hotel C, Dinkel J, et al. Non-contrast-enhanced perfusion and ventilation assessment of the human

lung by means of fourier decomposition in proton MRI. Magn Reson Med. 2009;62(3):656–64.
16. Bauman G, Bieri O. Matrix pencil decomposition of time-resolved proton MRI for robust and improved assessment of pulmonary ventilation and perfusion. Magn Reson Med. 2017;77(1):336–42.
17. Klimeš F, Kern AL, Voskrebenzev A, Gutberlet M, Grimm R, Müller RA, et al. Free-breathing 3D phase-resolved functional lung MRI vs breath-hold hyperpolarized 129Xe ventilation MRI in patients with chronic obstructive pulmonary disease and healthy volunteers. Eur Radiol. 2024. https://doi.org/10.1007/s00330-024-10893-3.
18. Marshall H, Voskrebenzev A, Smith LJ, Biancardi AM, Kern AL, Collier GJ, et al. 129Xe and Free-Breathing 1H ventilation MRI in patients with cystic fibrosis: A Dual-Center study. J Magn Reson Imaging. 2023;57(6):1908–21.
19. Hegi-Johnson F, de Ruysscher D, Keall P, Hendriks L, Vinogradskiy Y, Yamamoto T, et al. Imaging of regional ventilation: is CT ventilation imaging the answer? A systematic review of the validation data. Radiother Oncol. 2019;137:175–85.
20. Kipritidis J, Tahir BA, Cazoulat G, Hofman MS, Siva S, Callahan J, et al. The VAMPIRE challenge: A multi-institutional validation study of CT ventilation imaging. Med Phys. 2019;46(3):1198–217.
21. Ireland RH, Tahir BA, Wild JM, Lee CE, Hatton MQ. Functional Image-guided radiotherapy planning for normal lung avoidance. Clin Oncol. 2016;28(11):695–707.
22. Vinogradskiy Y, Castillo R, Castillo E, Schubert L, Jones BL, Faught A, et al. Results of a Multi-Institutional phase 2 clinical trial for 4DCT-Ventilation functional avoidance thoracic radiation therapy. Int J Radiat Oncol. 2022;112(4):986–95.
23. Baschnagel AM, Flakus MJ, Wallat EM, Wuschner AE, Chappell RJ, Bayliss RA et al. A Phase 2 Randomized Clinical Trial Evaluating 4-Dimensional Computed Tomography Ventilation-Based Functional Lung Avoidance Radiation Therapy for Non-Small Cell Lung Cancer. Int J Radiat Oncol Biol Phys [Internet]. 2024 Feb 20 [cited 2024 Jul 11];0(0). Available from: https://www.redjournal.org/article/S0360-3016(24)00327-4/abstract
24. Kipritidis J, Woodruff HC, Eslick EM, Hegi-Johnson F, Keall PJ. New pathways for end-to-end validation of CT ventilation imaging (CTVI) using deformable image registration. In: 2016 IEEE 13th International Symposium on Biomedical Imaging (ISBI). 2016. pp. 939–42.
25. Eslick EM, Bailey DL, Harris B, Kipritidis J, Stevens M, Li BT, et al. Measurement of preoperative Lobar lung function with computed tomography ventilation imaging: progress towards rapid stratification of lung cancer lobectomy patients with abnormal lung function. Eur J Cardiothorac Surg. 2016;49(4):1075–82.
26. Eslick EM, Kipritidis J, Gradinscak D, Stevens MJ, Bailey DL, Harris B, et al. CT ventilation imaging derived from breath hold CT exhibits good regional accuracy with Galligas PET. Radiother Oncol. 2018;127(2):267–73.
27. Eslick EM, Kipritidis J, Gradinscak D, Stevens MJ, Bailey DL, Harris B et al. CT Ventilation as a functional imaging modality for lung cancer radiotherapy (CT-vs-PET-Ventilation-Imaging) [Internet]. The Cancer Imaging Archive; 2022 [cited 2023 Feb 22]. Available from: https://doi.org/10.7937/3PPX-7S22
28. Clark K, Vendt B, Smith K, Freymann J, Kirby J, Koppel P, et al. The Cancer imaging archive (TCIA): maintaining and operating a public information repository. J Digit Imaging. 2013;26(6):1045–57.
29. Guerrero T, Sanders K, Noyola-Martinez J, Castillo E, Zhang Y, Tapia R, et al. Quantification of regional ventilation from treatment planning CT. Int J Radiat Oncol. 2005;62(3):630–4.
30. Kipritidis J, Siva S, Hofman MS, Callahan J, Hicks RJ, Keall PJ. Validating and improving CT ventilation imaging by correlating with ventilation 4D-PET/CT using 68Ga-labeled nanoparticles. Med Phys. 2014;41(1):011910.
31. Reinhardt JM, Ding K, Cao K, Christensen GE, Hoffman EA, Bodas SV. Registration-based estimates of local lung tissue expansion compared to Xenon CT measures of specific ventilation. Med Image Anal. 2008;12(6):752–63.
32. Bland JM, Altman DG. Statistical methods for assessing agreement between two methods of clinical measurement. Lancet. 1986;327(8476):307–10.
33. Crawford ABH, Makowska M, Engel LA. Effect of tidal volume on ventilation maldistribution. Respir Physiol. 1986;66(1):11–25.
34. Crawford AB, Cotton DJ, Paiva M, Engel LA. Effect of lung volume on ventilation distribution. J Appl Physiol. 1989;66(6):2502–10.
35. Paiva M, Van Muylem A, Ravez P, Yernault JC. Preinspiratory lung volume dependence of the slope of the alveolar plateau. Respir Physiol. 1986;63(3):327–38.
36. Tahir BA, Marshall H, Hughes PJC, Brightling CE, Collier G, Ireland RH, et al. Comparison of CT ventilation imaging and hyperpolarised gas MRI: effects of breathing manoeuvre. Phys Med Biol. 2019;64(5):055013.
37. Hughes PJC, Smith L, Chan HF, Tahir BA, Norquay G, Collier GJ, et al. Assessment of the influence of lung inflation state on the quantitative parameters derived from hyperpolarized gas lung ventilation MRI in healthy volunteers. J Appl Physiol. 2019;126(1):183–92.
38. Shin KM, Choi J, Chae KJ, Jin GY, Eskandari A, Hoffman EA, et al. Quantitative CT-based image registration metrics provide different ventilation and lung motion patterns in prone and supine positions in healthy subjects. Respir Res. 2020;21(1):1–9.
39. Mistry NN, Diwanji T, Shi X, Pokharel S, Feigenberg S, Scharf SM, et al. Evaluation of fractional regional ventilation using 4D-CT and effects of breathing maneuvers on ventilation. Int J Radiat Oncol. 2013;87(4):825–31.

Publisher's note